CONTINUOUS ACTIVATION ENERGY REPRESENTATION OF THE ARRHENIUS EQUATION FOR THE PYROLYSIS OF CELLULOSIC MATERIALS: FEED CORN STOVER AND COCOA SHELL BIOMASS

ABHISHEK S. PATNAIK[*] and JILLIAN L. GOLDFARB[*,**]

[*]*Division of Materials Science and Engineering, Boston University, 15 St. Mary's St., Brookline, MA 02446*
[**]*Department of Mechanical Engineering, Boston University, 110 Cummington Mall, Boston, MA 02215*
✉ *Corresponding author: Jillian L. Goldfarb, jilliang@bu.edu*

Received January 22, 2015

Kinetics of lignocellulosic biomass pyrolysis – a pathway for conversion to renewable fuels/chemicals – is transient; discreet changes in reaction rate occur as biomass composition changes over time. There are regimes where activation energy computed via first order Arrhenius function yields a negative value due to a decreasing mass loss rate; this behavior is often neglected in the literature where analyses focus solely on the positive regimes. To probe this behavior feed corn stover and cocoa shells were pyrolyzed at 10K/min. The activation energies calculated for regimes with positive apparent activation energy for feed corn stover were between 15.3 to 63.2 kJ/mol and for cocoa shell from 39.9to 89.4 kJ/mol. The regimes with a positive slope (a "negative" activation energy) correlate with evolved concentration of CH_4 and C_2H_2. Given the endothermic nature of pyrolysis, the process is not spontaneous, but the "negative" activation energies represent a decreased devolatilization rate corresponding to the transport of gases from the sample surface.

Keywords: Arrhenius equation, biomass pyrolysis, evolved compounds, activation energy

INTRODUCTION

Fossil fuels comprise the majority of the total energy supply in the world today.[1]One of the most critical areas to shift our dependence from fossil to renewable fuels is in energy for transportation, which accounts for well over half of the oil consumed in the United States. The Renewable Fuel Standard (RFS2) of the Energy Independence and Security Act of 2007 mandates that 16 billion gallons of a cellulosic biofuel, achieving a 60% reduction in greenhouse gas emissions, be blended into transportation fuels by 2022. A portion of this biofuel must be biodiesel produced from biomass.[2] Many processes to convert biomass to liquid fuels rely on pyrolysis, the thermal decomposition of a solid fuel in the absence of oxygen. One of the challenges facing the sustainable production of renewable energy sources such as biomass is to develop an understanding of the reaction kinetics when the biomass is thermochemically converted to biofuel.

There are multiple methods used to analyze the pyrolysis kinetics of solid carbonaceous fuels, the overwhelming majority of which rely on the Arrhenius equation, expressed in the general form as:

$$k = Ae^{-E_a/RT} \quad (1)$$

where A is the frequency (or pre-exponential) factor, E_a the activation energy, T the absolute temperature, R the universal gas constant, and k is the is the reaction rate constant. It is common to assume that the pyrolytic decomposition of biomass and other carbonaceous fuels proceeds according to an infinitely large set of first order reactions, allowing for the calculation of an overall, or apparent activation energy assuming an overall first order reaction (or a series of reactions that sum to an overall first order reaction). Innumerable studies in the biomass pyrolysis literature calculate this activation energy using

this assumption, also known as the Reaction Rate Constant Method (RRCM).[3,4] Dozens of biomass pyrolysis studies in the literature show a reaction order of approximately unity. This assumption is commonly applied to account for the simultaneous reactions occurring during the pyrolysis of heterogeneous biomasses and is considered a reasonable approximation given the high degree of linearity of the Arrhenius plots.[2,5] Therefore, it provides a useful basis of comparison for the pyrolysis of different biomasses and other solid fuels in the literature.

However, despite the highly linear relationships encountered for biomass pyrolysis, the RRCM fails to capture the entire range of decomposition. For biomass pyrolysis we commonly see multiple mass loss regimes over different temperature ranges accounting for the stage-wise decomposition of the primary biomass constituents. That is, the Arrhenius plots have discrete changes in slope that occur over specific (though similar) temperature ranges for each biomass. For example, using the RRCM, our laboratory found three primary decomposition regions for the pyrolysis of cabbage palm (*Sabal palmetto*), likely corresponding to devolatilization of primarily hemicellulose, cellulose and lignin.[4] However, we know that lignin can devolatilize over a broad temperature range,[7] which the limited "mass loss regime" approach of the RRCM cannot differentiate. In addition, though the changes in slope in the ln(k)vs. $1/T$ Arrhenius plots are fairly straightforward to analyze, there can be substantial (between 2 and 20%) mass lost between one "regime" and another depending on the temperature ramp rate and the temperature range selected for analysis, which is not captured in the RRCM analysis. Selecting a temperature range that encapsulates the most mass loss will decrease the linearity of the mass loss regime due to curvature of the line at tail ends, leading to the inability to completely capture the entire conversion in such an analysis. In their critical review of the application of the Arrhenius equation to solid-state kinetics, Galwey and Brown[8] succinctly summarize why we continuously apply the Arrhenius equation to such systems. "No realized alternative capable of expressing the form of the k-T relationship or providing an explanation of this pattern of behavior has gained acceptance."

When analyzing the pyrolytic decomposition process of a biomass across a broad decomposition temperature range using the Arrhenius equation (ln(k) vs. $1/T$), we see multiple discreet changes in the slope of the curve equating to changes in the reaction rates leading to segmentation of the process into multiple regimes of decompositions. However, there are intermediate regimes wherein the slope of the Arrhenius plot changes from negative to positive, equating to negative activation energy. It is not clear that this represents a "spontaneous" pyrolysis reaction as one would associate with negative activation energy. More likely, it is simply the decrease in reaction (mass loss) rate as the biomass is depleted of one constituent at a lower temperature, before the decomposition of a more energy intensive component(s) begins at a higher temperature. This is perhaps an important distinction often overlooked in the literature; a complete understanding of the pyrolysis process of biomasses may enable better temperature range specifications for energy input, targeting the low activation energy regimes to maximize energy savings and product yield. Given the push towards lower energy consumption through the design of efficient industrial thermochemical conversion processes, it becomes imperative to understand the decomposition kinetics of the entire pyrolysis process. If there are regimes in which a mass loss rate decreases substantially despite additional heat input, such a process may require less energy to yield a similar product. This paper presents an investigation of the pyrolysis kinetics of two common biomasses, feed corn stover and cocoa shell, applying a novel empirical approach developed to analyze the transient nature of pyrolysis through the changing slopes of the Arrhenius plot.

EXPERIMENTAL

Materials

Feed corn stover is a seasonally available feedstock, grown across the United States. It is estimated that there is approximately 1 dry ton of harvestable stover per acre of planted corn.[9] According to the National Corn Grower's Association, 97.2 million acres of corn were planted in 2012, almost 4 million of which were in the Northeast and Mid-Atlantic states.[10] Feed corn stover samples were collected early in October 2011 from the Coppal House Farm in Lee, NH; the stalk and residual leaves were comingled. To prevent it from decomposing, the feed corn stover was dried in a laboratory oven immediately after collection and stored in airtight containers.

According to the World Cocoa Foundation, total cocoa production was up 8.73% from 2008 to 2012,

with 400 tons of cocoa beans ground and processed in the United States in 2011-2012, representing approximately 10% of the world's grindings.[11] Cocoa bean shells exit the chocolate process as a dry stream; samples obtained from Lindt Chocolate, Stratham, NH, after removal of the cocoa nib were stored in airtight containers as received.

Table 1
Ultimate and proximate analyses of feed corn stover and cocoa bean shell samples

Wt% (Dry basis)	Cocoa bean shells	Feed corn stover
C	47.04	46.55
H	5.43	5.66
N	2.79	0.95
S	0.16	0.13
O	35.59	39.59
Ash	9.00	7.12
Moisture	3.59	4.54

Both biomasses were ground and sieved to a particle size fraction of less than 125 µm. Table 1 gives the ultimate and proximate analyses for each of these materials, performed by LECO Analytical.

Activation energy calculation from thermogravimetric analysis

The mass loss behavior of the two biomasses was characterized using thermogravimetric analysis (TGA). The feed corn and the cocoa shells were pyrolyzed in high purity nitrogen at a flow of approximately 50 mL/min in a 70 µL alumina crucible in a Mettler Toledo TGA/DSC1 with a 20 mL/min high purity nitrogen stream to protect the balance. Mass and temperature were recorded every second to the 10^{-8} grams and ±0.1 K, respectively. The biomasses were of a particle size less than 125µm to insure that the Biot number (Bi) is considerably less than one, in order to negate transport limitations caused by large particles, as given by Equation (2):

$$Bi = \frac{hl}{\lambda} \quad (2)$$

where l is the particle's characteristic length (estimated here as the particle size of 125 µm); h is the convection coefficient; λ is the thermal conductivity of the biomass. As an order of magnitude estimate, if we assume that the thermal conductivity of biomass particles ranges from 0.01 to even as high as 1.0 W/mK, and the convection coefficient ranges from 0.25 to 1 W/m^{2}K,[12,13] we find a Biot number in the conservative range of $3*10^{-5}$ to 0.1, negating internal transport resistances. This was experimentally validated by measuring the activation energies of biomass particles of less than 500 µm in size with no observed impact of particle size on E_a.[4] The sample size was maintained at approximately 5-7 mg to minimize potential heat and mass transfer limitations within the crucible. All samples were initially heated to 373 K and held for 30 minutes to insure moisture removal. The temperature was ramped back down to 298 K at 10 K/min and held for 5 minutes. Then the sample was heated at 10 K/min up to 1020 K and held for 60 minutes to obtain a stable mass reading. The DSC (Differential Scanning Calorimeter) was calibrated with indium at a rate of 10 K/min. Each sample was run a minimum of three times to insure reproducibility.

The apparent activation energy of biomass pyrolysis was calculated using the Arrhenius equation under the assumption of overall first order reaction kinetics using the mass loss function. The rate of material decomposition is given as:

$$\frac{dX(t)}{dt} = k(1 - X(t)) \quad (3)$$

$X(t)$ represents the extent of conversion at any time, t, calculated by the ratio of the mass of volatiles produced at any given time, equating to the initial mass, m_0, minus the mass at time t, m_t, to the total volatiles produced at the end of the pyrolysis reaction, $m_0 - m_f$, where m_f is the final mass at the end of the pyrolysis process. $X(t)$ is given by:

$$X(t) = \frac{m_0 - m_t}{m_0 - m_f} \quad (4)$$

For non-isothermal experiments, the sample temperature is expressed as:

$$T = T_0 + \beta t \quad (5)$$

where T_0 is the initial absolute temperature and β is the constant heating rate (β=dT/dt). Using the chain rule on Eq. (3) and by rearranging, k may be solved for as:

$$k = \beta \frac{dX(T)}{dT} \Big/ (1 - X(T)) \quad (6)$$

Manipulating equation (1) we get equation (7), which is essentially a linear function of $ln(k)$ with respect to $1/T$. Therefore, a plot of $ln(k)$ *vs.* $1/T$ should yield a straight line if the reaction order is one. The apparent activation energy, E_a can be calculated from the slope (slope= $-E_a/R$) and the frequency factor, A, from ordinate intercept (y-intercept =$ln(A)$).

$$\ln(k) = \ln(A) - \frac{1}{T}\frac{E_a}{R} \quad (7)$$

The plot of [–R*$d(ln(k))$]/[$d(1/T)$]vs. $1/T$ yields a continuous curve of the apparent activation energy, E_a as a function of inverse temperature. This continuous plot will be used to illustrate the transient nature of the pyrolysis reaction of the biomasses.

Devolatilized gas species analysis from quadrupole mass spectrometry (QMS)

The devolatilized species from biomass pyrolysis were analyzed in a separate experiment. This was done in order to increase the signal to noise ratio as a much higher mass of the biomass can be used in a tube furnace as compared to the TGA. The biomass was pyrolyzed in a one inch diameter tube furnace (Lindberg/Blue M® - Mini-Mite™) fitted with a quartz tubular reactor, under a high purity stream of nitrogen at a flow rate of approximately 100 mL/min as measured by a digital Omega flowmeter calibrated for N_2. Samples of approximately 0.45 g were placed in a porcelain boat at the center of the hot zone of the furnace, reaching the same relative height in the porcelain boat as in the TGA's crucible. A temperature ramp rate of 10 K/min was used to avoid any diffusion effects arising from heat transfer and to mirror the TGA experiments. Samples were initially soaked at 373 K for 30 minutes to insure moisture removal. The exhaust was directed to a fused silica capillary tubing (40µm inside diameter) which was connected to a Quadrupole Mass Spectrometer (Extorr XT Series RGA, XT300M) for analysis. The mass spectrometer was in the electron impact (EI) ionization mode at the electron energy of 70 eV and provided mass spectra up to 300 a.m.u. Figure 1 is a schematic for the set-up. Using a mass spectrometer to measure evolved gases from pyrolysis is commonly employed in the literature; they are often connected directly to a TGA.[14] With the tube furnace set-up we were able to use larger samples than in the TGA, and were able to see compound evolving at lower concentrations than the small TGA sample sizes allow.

Two pyrolysis mass spectrum runs were performed on the biomass initially to identify the significant species devolatilizing throughout the pyrolysis process. Subsequently "trend scans" were used to monitor significant species detected in the full spectrum runs in order to trace their devolatilization trend throughout the pyrolysis process. A dwell time of 100 ms was used for each a.m.u scanned. This article primarily studies the mass spectra of 2, 14, 16, 18, 26, 28, 29, 32, 44 a.m.u, which are assigned to H_2, CH_2, CH_4, H_2O, C_2H_2, $N_2/CO/C_2H_4$, C_2H_5, O_2, and CO_2, respectively. The concentration versus temperature trend of each species in conjunction with the TGA data was then used for further analysis of the pyrolysis behavior.

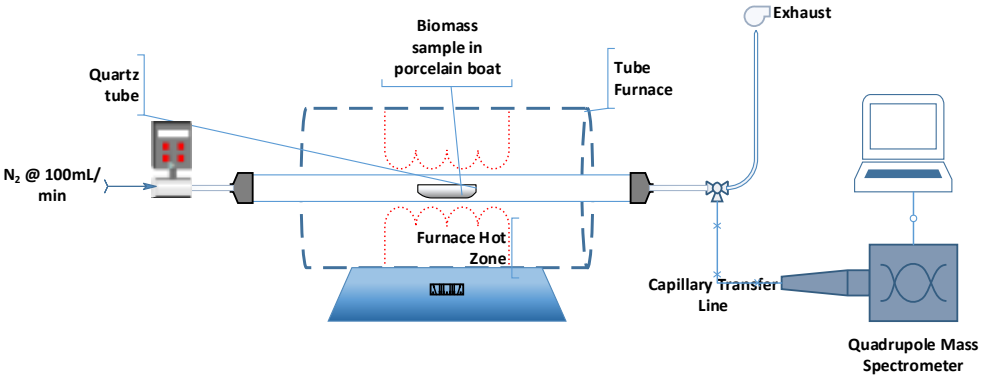

Figure 1: Schematic of the QMS measurement set-up used to monitor evolved gases during pyrolysis at 10 K/min

RESULTS AND DISCUSSION

In this study, a continuous representation of the apparent activation energy (computed from the Arrhenius equation) in conjunction with the concentration trends of the devolatilized species is used to illustrate the transient nature of the kinetics of the pyrolysis process across the entire mass loss temperature regime. One objective is to determine if a correlation exists between concentration trend of specific species and the changes in the activation energy over the entire mass loss regime of the biomass. To this end, separate experiments of TGA and QMS were performed across two biomass samples, feed corn stover and cocoa shell.

Analysis of thermogravimetric data

The feed corn stover and cocoa shell biomasses were pyrolyzed in the TGA at a temperature ramp rate of 10 K/min three times each to insure reproducibility. Figures 2(a) and

(b) show the mass loss versus sample temperature of the biomasses (only one run is plotted for each for readability). These figures also overlay the derivative thermogravimetry (DTG) plot for the biomass showing the mass loss rate (d(*wt*%)/d*T*) versus temperature. The combined plots of the three runs for each biomass are shown in Figure 3. The onset of mass loss for feed corn stover occurred at 428.15 ± 1.64K and for cocoa shell at 420.77 ± 0.53 K. The residual mass after pyrolysis for feed corn stover was 32.58 ± 1.64 wt%, while that for the cocoa shell was 33.07 ± 0.21 wt%. Note that the residual mass values for feed corn stover and cocoa shell are higher than those reported in the literature as the referenced studies also account for the loss in weight from desorption of physisorbed water apart from the fact that each biomass source has an inherent variability in constitution.[15-21] The physisorbed water content for feed corn stover was 4.54 wt% and that for cocoa shells was 3.59 wt%; the kinetic analysis is performed on dry samples to remove moisture variability across samples.

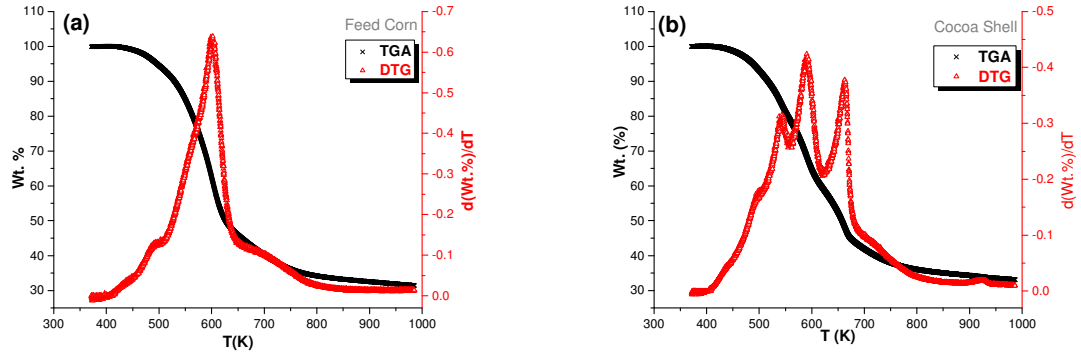

Figure 2: TGA/DTG plot for (a) feed corn stover and, (b) cocoa shell. The black curve (×) represents the TGA plot and the red curve (Δ) represents the DTG plot

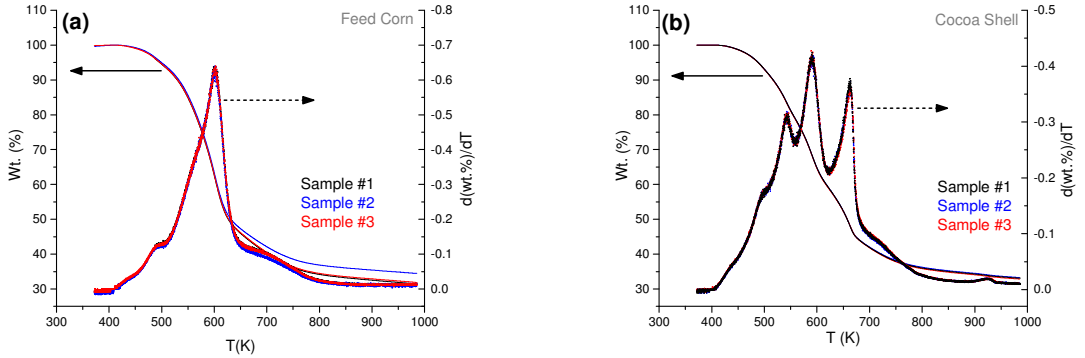

Figure 3: TGA/DTG plot of the three samples for (a) feed corn stover and (b) cocoa shell

The TGA plot shows that in the case of feed corn stover the highest mass loss rate regime is from 530 K to 630 K, losing 40.50 ± 0.29% of total dry sample mass while that for cocoa shell is 475 K to 671 K, losing 51.16 ± 0.05% of total dry sample mass. The derivative thermogravimetric (DTG) curves in Figure 2 show the mass loss rate as a function of temperature. In case of feed corn stover we find one large peak at 603 K, a small shoulder at 487 K, and a plateau between ~650 and 750 K. The large and small peaks are in good agreement with the literature,[15-19] accounting for minor variations in samples such as source, species of corn, particle size and any pre-treatment methods. The cocoa shell has three prominent peaks at 542 K, 590 K and 662 K and three minor shoulders at 496 K, 718 K and 926 K. These peaks match closely with what was seen by Du *et al.*[20] and Pereira *et al.*[21].

Biomass has three primary components namely, cellulose, hemicellulose and lignin. The quantity of each component will vary depending on the type and source of the biomass. Most biomass sources contain approximately 30-60% cellulose, 25-35% hemicellulose and 15-30% lignin.[7,15,22-26] Yang *et al.*[24] found the decomposition of hemicellulose occurs at 493-588 K, cellulose at 588-673 K and lignin over the broad range of 433-1173 K. The variation of these fundamental components across biomass samples causes different responses to pyrolytic treatments. As can be seen from Figure 2(a), the main DTG peak at 603 K of feed corn stover likely corresponds to cellulose decomposition since cellulose is the dominant component, and the low temperature shoulder peak (487 K) can likely be attributed to hemicellulose.[7,22-24]

Table 2
Activation energy, frequency factor and mass loss percent across each mass loss regimes for pyrolysis of feed corn stover and cocoa shell determined using first order Arrhenius equation (confidence interval represents standard deviation of three averaged runs)

Biomass	Onset T (K)	Endset T (K)	E_a (kJ/mol)	A (1/s)	Mass loss (wt%)
Feed corn stover	454.33 ± 0.38	493.91 ± 0.09	51.84 ± 0.85	112.33 ± 24.48	3.54 ±0.12
	510.09 ± 0.25	608.98 ± 0.12	62.52 ± 1.05	850.43 ± 219.11	35.93 ± 0.15
	658.18 ± 0.21	730.52 ± 0.36	15.25 ± 2.19	0.02 ± 0.01	7.17 ± 0.44
	894.84 ± 0.36	981.93 ± 2.66	63.16 ± 11.36	7.81 ± 7.00	1.14 ± 0.13
Cocoa shell	454.55 ± 0.00	543.98 ± 0.12	39.94 ± 0.04	6.86 ± 0.07	15.39 ± 0.13
	562.10 ± 0.09	593.60 ± 0.19	68.86 ± 0.27	2356.43 ± 124.63	10.50 ± 0.61
	619.39 ± 0.17	665.42 ± 0.06	89.41 ± 0.61	38822.54 ± 4841.85	12.00 ± 0.08
	866.48 ± 2.98	924.80 ± 0.13	87.88 ± 1.17	179.32 ± 24.79	0.91 ± 0.01
	939.20 ± 0.38	980.39 ± 0.00	64.34 ± 2.30	6.45 ± 1.79	0.55 ± 0.05

In addition, a contribution from lignin decomposition, which takes place over a broad temperature range with low mass loss rate, is represented by the high temperature plateau (650-750 K). In the case of cocoa shell, (Figure 2(b)), the peaks in the range of 513-653 K are likely attributed to the degradation of cellulose and hemicellulose and those in the range of 673-793 K to the degradation of lignin.[21] Pereira *et al.*[21] attribute the fluctuations above 873 K to "prolonged lignin degradation since this compound has high stability." Du *et al.*[20] note that cocoa shell contains varying amounts of pectic polysaccharides, theobromine and fats in addition to the hemicellulose, cellulose and lignin, which will undergo thermal decomposition alongside the hemicellulosic components, and thus the DTG peaks cannot be exclusively assigned to any particular component.

Analysis of apparent activation energy

The TGA data for feed corn stover and cocoa shell biomasses were manipulated as explained previously to obtain a continuous Arrhenius plot spanning the entire pyrolysis temperature range. Figure 4(a) and (b) show these plots for feed corn stover and cocoa shell biomasses respectively pyrolyzed at 10 K/min. The Arrhenius plots are segmented into multiple regimes characterized by a negative slope. A linear fit is used for each regime to calculate the apparent activation energy (E_a) and frequency factor (A). These regimes for feed corn stover and cocoa shell are shown in Table 2. Feed corn stover pyrolysis is divided into four regimes: 454-494 K, 510-609 K, 658-730 K and, 895-982 K. The activation energies for these regimes are 51.84±0.85, 62.52±1.05, 15.25±2.19 and 63.16±11.36 kJ/mol respectively. Cocoa shell pyrolysis is divided into five regimes: 455-544 K, 562-594 K, 620-665 K, 866-925 K and 939-980 K. The activation energies for these regimes were 39.94±0.04, 68.86±0.27, 89.41±0.61, 87.88±1.17 and 64.34±2.30 kJ/mol respectively. The apparent activation energy values are in the same range as reported in the literature,[15-21] albeit the selection method of the regimes is different in this study. Here we segment each regime based on the slope of the Arrhenius curve, whereas the referenced studies segment the regimes based on the TGA graphs representing the regime of highest mass loss of dry biomass. The activation energy for feed corn stover, if determined in this

manner, was 51.36±2.09 kJ/mol and that for the cocoa shell was 28.88 ±0.19 kJ/mol, in good accord with literature values. However, the application of the RRCM to these biomasses only accounts for ~48% of the total feed corn mass lost and 39% of the coca shell, whereas ~68wt% of the feed corn and ~67wt% of the cocoa shells decomposed during the entire pyrolysis process. Thus, the RRCM is only accounting for 71% and 58% of the total mass loss of the feed corn and cocoa shells, respectively, in the regimes in which we see highly linear, positive activation energies. As such, we turn our attention to the portions of the Arrhenius plot that are neglected in a traditional RRCM analysis.

The Arrhenius plots, Figure 4 (a) and (b), for each biomass show regimes with a positive slope (marked by a dashed circle on the plot) which, according to Equation 1, yields a negative activation energy. Feed corn stover pyrolysis has two such regimes in the 610-650 K and 680-810 K temperature range while cocoa shell has four such regimes in the 545-555 K, 590-620 K, 670-850 K and 950-960 K temperature ranges. A change in slope in the Arrhenius plot from negative to positive occurs when the rate of mass loss decreases with an increase in temperature. Such behavior has been seen in reactions ranging from organo-catalytic processes, gas phase reactions to stratospheric ozone depletion and interstellar chemistry.[27-33] Essentially, all the referenced articles conclude that the observance of negative activation energy for an addition reaction entails a two-step process where the activation energy of one of the steps becomes negative (spontaneous), while the activation energy of the other step remains low, thus making the total sum negative. Pyrolysis, on the other hand, is essentially an endothermic process comprising multiple dissociation reactions of polymer chains occurring at a given instant.[23] Hence the arguments drawn from the interpretation of addition reactions showing negative activation energy cannot be used for pyrolytic dissociation reactions. Because of the heterogeneous nature of the biomass samples and multiple simultaneous reactions known to occur in biomass pyrolysis,[34-36] we cannot use any single dissociation reaction to describe the evolving nature of the Arrhenius plot. As such, we probe whether or not the changes in concentration of the marker species tracked during evolution can be used as an indicator to describe the portions of the Arrhenius plot where the dissociation rate decreases with increasing temperature in certain temperature regimes. In an attempt to recognize such a hypothesis, we compile data from the two experiments, namely (1) pyrolysis rate as a function of temperature using a TGA and, (2) devolatilized gaseous products of the pyrolysis process real-time by the use of a quadrupole mass spectrometer. The objective was to find if the concentration profiles of any devolatilized species correlates with the temperature regimes where the dissociation rates decrease with increasing temperature.

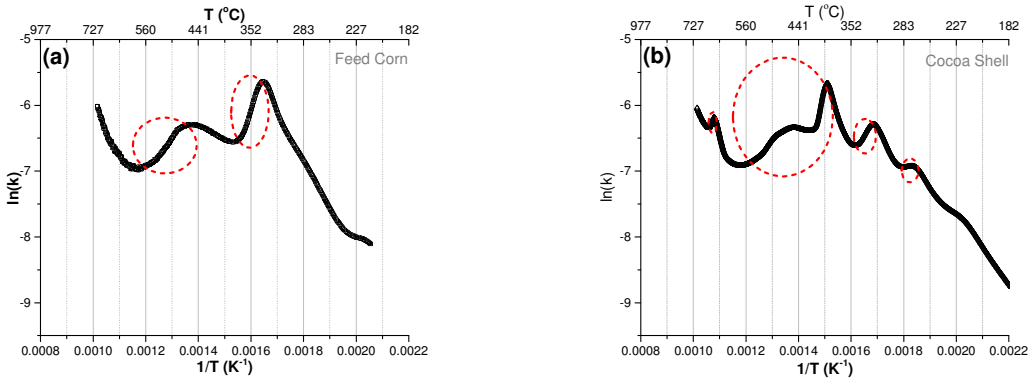

Figure 4: Arrhenius plot for (a) feed corn stover and, (b) cocoa shell. Dashed circles are used to identify the regions with positive slope, which translate to negative apparent activation energies

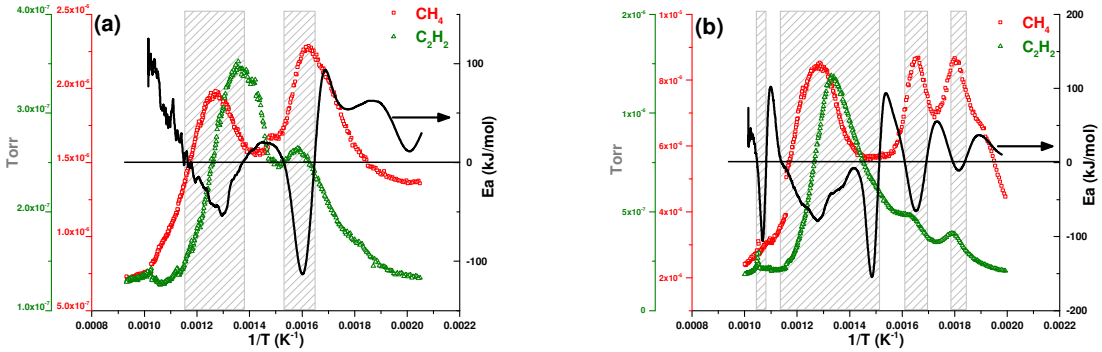

Figure 5:Continuous plot of the apparent activation energy (—) overlaid with the concentration profiles of CH_4 (□) and C_2H_2 (Δ) for (a) feed corn stover and (b) cocoa shell. The solid horizontal line denotes zero activation energy. The hatched areas denote regimes with negative activation energy

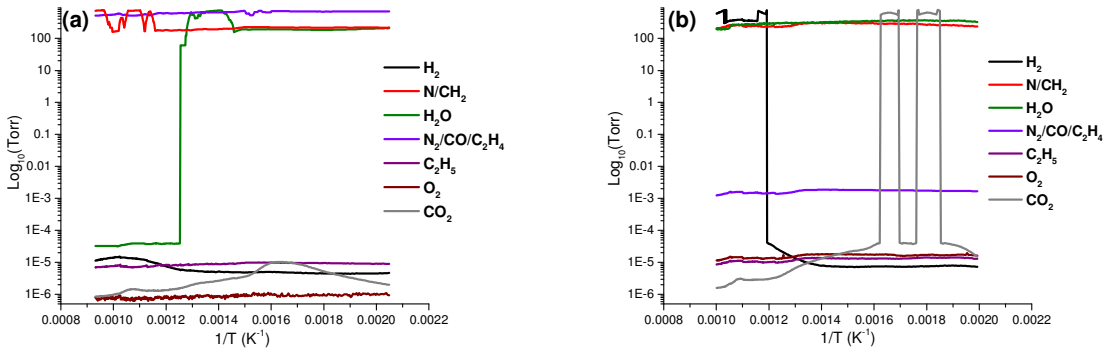

Figure 6: Concentration trend of H_2 (Black), CH_2 (Red), H_2O (Green), $N_2/CO/C_2H_4$ (Violet), C_2H_5 (Purple), O_2 (Wine), and CO_2 (Gray) as a function of inverse temperature for (a) feed corn stover and (b) cocoa shell.A filter was applied to smooth noise in the trend data for H_2, N/CH_2 and H_2O

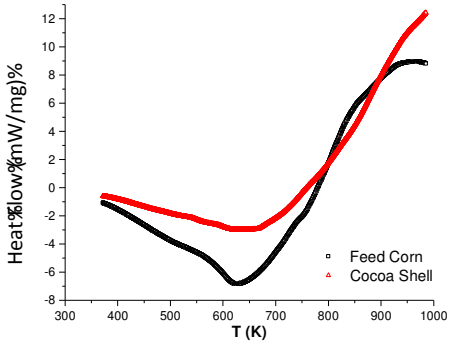

Figure 7: DSC plot of feed corn stover (black, □) and cocoa shell (red, Δ) pyrolysis

Equation (7) was used to plot the Arrhenius curve for the pyrolysis of feed corn stover and cocoa shell represented in Figures 4(a) and 3(b). The derivative of the Arrhenius plot representing the apparent activation energy, E_a, as a function of inverse temperature is shown in Figures 5(a) and 4(b) for feed corn stover and cocoa shell, respectively. The continuous activation energy plots are overlaid with the concentration of evolved gases (as measured by partial pressure) obtained from the quadrupole mass spectrometer. Among the species scanned by the mass spectrometer over the pyrolysis temperature range, CH_4 and C_2H_2, increased in concentration

in the same temperature regimes as the so-called negative activation energy regimes, or those regimes in which the rate of mass loss decreased as temperature increased. The concentration profiles as a function of the other species scanned are shown in Figures 6 (a) and (b).

In the case of feed corn stover where we observe two such regimes between 610-650 K and 680-810 K, all three species show an increase in concentration. In the case of cocoa shell, the concentration of the same three species increases in all the four regimes (545-555 K, 590-620 K, 670-850 K and, 950-960 K). The alignment of the peaks of concentrations of CH_4 and C_2H_2 to that of the negative activation energy regimes likely indicates one of the following behaviors. First, the activation energy could be negative – that is, there may be regimes of spontaneous reaction occurring during pyrolysis – one could envision this as a synergistic effect among the biomass constituents whereby depolymerization of chains occurs in one component, such as cellulose, leading to spontaneous disruption of the lignin matrix. However, this is an unlikely scenario; these negative activation energy regimes are *not* indicative of spontaneous chemical reactions occurring. We can draw this conclusion looking at Figure 7, plotting the results of the DSC scans taken during pyrolysis of the samples. The pyrolysis of both feed corn and cocoa shells are endothermic throughout this decomposition temperature range; that is, heat is required to pyrolyze the samples.

The second option to explain this "negative" E_a behavior is to consider the physicality of the pyrolysis of heterogeneous samples such as biomass. The RRCM is often applied to these samples and yields multiple "regimes," wherein the slope of the Arrhenius plot is highly linear and yields positive activation energy. The temperature, length, and slope of these regimes depend on the specific biomass. The portions of the Arrhenius plot not considered a part of these regimes are neglected because the activation energy tends "negative," and the linearity of the plot is severely compromised. During these times, the mass loss rate decreases, which leads to the negative E_a as computed through Equation 7. This brings us to the spike in concentration of marker evolved gas compounds such as CH_4 and C_2H_2. There is a short delay (on the order of 5seconds) between the moment the sample devolatilizes and when the compounds are detected in the MS. The peaks of concentrations align well with the trough of the activation energy curve, as seen in Figure 5, suggesting that the mass loss rate declines after the volatiles that can be lost in a given temperature range peak.

CONCLUSION

Thermogravimetry in conjunction with quadrupole mass spectrometry of feed corn stover and cocoa shell biomass pyrolysis was used to investigate the transient nature of biomass pyrolysis and the application of the first order Arrhenius equation. The TGA plots show that the feed corn stover and cocoa shell have a residual weight of 32.58 ± 1.64 wt% and 33.07 ± 0.21 wt% respectively after pyrolysis. The overall pyrolysis reaction of feed corn stover was divided into four regimes based on a negative slope of the Arrhenius plot. The activation energies were found to be in the range of 15.25 to 63.16 kJ/mol. Similarly, cocoa shell pyrolysis was divided into five regimes with activation energies ranging from 39.94to 89.41 kJ/mol. The continuous function of the Arrhenius equation (assuming reaction order of unity) encompassing the entire range of pyrolysis reaction for the two biomasses, revealed regimes of positive slopes (slowing reaction rates) equating to negative apparent activation energy values. Real-time analysis of the devolatilized products of the pyrolysis process revealed that gaseous species such as CH_4 and C_2H_2 increase in concentration in the same temperature regime where the reaction rate decreases with increasing temperature. It was noted that the same three devolatilized species were observed to increase in concentration for both the biomasses. These species can be used as marker compounds to identify spontaneous reaction regimes in the pyrolysis of ligno-cellulosic biomasses, enabling the design of more energy efficient industrial thermochemical processes. By specifying process temperatures that maximize volatile production without increasing temperature beyond which the reactions rates decrease, we can improve the overall pyrolysis process.

ACKNOWLEDGEMENTS: This material is based upon work supported by the National Science Foundation under Grant No. NSF CBET-1127774.

REFERENCES

[1] A. Demirbas, "Biodiesel: A Realistic Fuel Alternative for Diesel Engines", Springer-Verlag London Ltd., London, U.K., 2008.

[2] N. Kauffman, D. Hayes, R. Brown, *Fuel*, **90**, 3306 (2011).

[3] P. Yangali, A. M. Celaya, and J. L. Goldfarb, *J. Anal. Appl. Pyrol.*,**108**, 203 (2014).

[4] L. Buessing, and J.L. Goldfarb, *J. Anal. Appl. Pyrol.*, **96**, 78 (2012).

[5] C. Branca, and C. Di Blasi, *J. Anal. Appl. Pyrol.*, **67**, 207 (2003).

[6] P. Parasuraman, R. Singh, T. Bolton, S. Omori and R. Francis, *BioResources*, **2** ,459 (2007).

[7] M. Brebu and C. Vasile, *Cellulose Chem. Technol.*, **44**,353 (2010).

[8] A.K. Galweyand M.E. Brown, *Thermochim. Acta*, **386**, 91 (2002).

[9] D. Petrolia, *Biomass Bioenerg.*, **32**, 603 (2008).

[10] National Corn Growers Association: http://www.ncga.com/upload/files/documents/pdf/WOC%202013.pdf, Date Accessed: 01/13/2015.

[11] World Cocoa Foundation, "Cocoa Market Updated as of 3-20-2012".http://worldcocoafoundation.org/wp-content/uploads/Cocoa-Market-Update-as-of-3.20.2012.pdf, Date Accessed: 01/13/2015.

[12] S. R. Gubba, L. Ma, M. Pourkashanian and A. Williams, *Fuel Proc.Technol.*, **92**, 2185 (2011).

[13] C. Di Blasi,*Fuel*,**76**, 957 (1997).

[14] Y. F. Huanga, W. H. Kuanb, P. T. Chiuehaand, S. L. Lo, *Bioresour. Technol.*, **102**, 3527 (2011).

[15] A. Kumara, L. Wanga, Y. A. Dzenisc, D. D. Jonesa and M.A. Hannaa, *Biomass Bioenerg.*, **32**, 460 (2008).

[16] Q. Cao, K. Xie, W. Bao, and S. Shen, *Bioresour. Technol.*, **94**, 83 (2004).

[17] G. Lv, and S. Wu, *J. Anal. Appl. Pyrol.*, **97**, 11 (2012).

[18] X. Zhang, M. Xu, R. Sun and L. Sun, *J. Eng. Gas Turbines Power,***128**, 493 (2006).

[19] Z. Q. Li, W. Zhao, B. H. Meng, C. L. Liu, Q. Y. Zhu *et al.*, *Bioresour. Technol.*,**9 9**, 7616 (2008).

[20] Y. Du, X. Jiang, G. Lv, X. Li, Y. Chi *et al.*, *J. Therm. Anal. Calorim.*, **117**, 343 (2014).

[21] R. G. Pereira, C. M. Veloso, N. Mendes da Silva, L. F. de Sousa, R. C. Ferreira Bonomo *et al.*, *Fuel Proc. Technol.*,**126**, 476 (2014).

[22] R. S. Miller and J. Bellan, *Combust. Sci. Tech.*, **126**, 97 (1997).

[23] M. Van de Velden, J. Baeyens, A. Brems and R. Dewil, *Renew. Energ.*, **35**, 232 (2010).

[24] H. Yang, R. Yan, H. Chen, D. H. Lee and C. Zheng, *Fuel*, **86**, 1781 (2007).

[25] S. D. Stefanidis, K. G. Kalogiannis, E. F. Iliopoulou, C. M. Michailof, P. A. Pilavachi *et al.*, *J. Anal. Appl. Pyrol.*, **105**, 143 (2014).

[26] G. Dorez, L. Ferry, R. Sonnier, A. Taguet and J.-M. Lopez-Cuesta, *J. Anal. Appl. Pyrol.*,**107**, 323 (2014).

[27] X. Han, R. Lee, T. Chen, J. Luo, Y. Lu *et al.*, *Scientific Reports*, **3**, 2557 (2013).

[28] L. E. Revelland, B. E. Williamson, *J. Chem. Educ.*, **90**, 1024 (2013).

[29] J. Wei, *Chem. Eng. Sci.*, **51**, 2995 (1996).

[30] A.S. Cukrowskia and M. A. Telka, *Chem. Phys. Lett.*, **297**, 402 (1998).

[31] J. Connor, R. W. Van Roodselaar, R.W. Fair and O. P. Strausz, *J. Am. Chem. Soc.*, **93**, 560 (1971).

[32] A. Menon, and N. Sathyamurthy, *J. Phys. Chem.* **85**, 1021 (1981).

[33] M. E. Davis and R. J. Davis, "Fundamentals of Chemical Reaction Engineering", McGraw Hill, New York, 2003.

[34] D. F. Arseneau, *Can. J. Chem.*, **49**, 632(1971).

[35] B. B. Uzun, A. E. Pütün and E. Pütün, *J. Anal. Appl. Pyrol.*, **79**, 147 (2007).

[36] M. S. Mettler, A. D. Paulsen, D. G. Vlachos and P. J. Dauenhauer, *Energ. Environ. Sci.*, **5**, 7864 (2012).